

Focused Ion Beam-Based Specimen Preparation for Atom Probe Tomography

Ji Yeong Lee, Jae-Pyoung Ahn*

Advanced Analysis Center, Korea Institute of Science and Technology (KIST), Seoul 02792, Korea

Currently, focused ion beams (FIB) are widely used for specimen preparation in atom probe tomography (APT), which is a three-dimensional and atomic-scale compositional analysis tool. Specimen preparation, in which a specific region of interest is identified and a sharp needle shape created, is the first step towards successful APT analysis. The FIB technique is a powerful tool for site-specific specimen preparation because it provides a lift-out technique and a controllable manipulation function. In this paper, we demonstrate a general procedure containing the crucial points of FIB-based specimen preparation. We introduce aluminum holders with moveable pin and an axial rotation manipulator for specimen handling, which are useful for flipping and rotating the specimen to present the backside and the perpendicular direction. We also describe specimen preparation methods for nanowires and nanopowders, using a pick-up method and an embedding method by epoxy resin, respectively.

*Correspondence to:
Ahn JP,
Tel: +82-2-958-5536
Fax: +82-2-958-6974
E-mail: jpahn@kist.re.kr

Received December 1, 2015
Revised December 16, 2015
Accepted December 16, 2015

Key Words: Atom probe, Focused ion beams, Specimen preparation, Lift-out technique

INTRODUCTION

Atom probe tomography (APT) provides the highest spatial resolution (0.24 nm) and high analytical sensitivity (10 appm) over meaningful sample volumes, and has a detection efficiency of 38%. Investigation by APT provides a three-dimensional view of the internal structure of an object, quantitative information for hydrogen and lithium, and analysis of atomic clustering.

The current most common geometry is the local electrode atom probe (LEAP), which first appeared commercially in 2002 (Kelly et al., 2004). It is named for the electrode which is positioned near a sample and, along with a position sensitive detector, forms an imaging system for ions emitted under voltage or laser pulsing. One version of this instrument, which first appeared in 2005, had a focused small-spot laser beam with a 10 μm diameter at the target; it is now in its second generation with a $<3 \mu\text{m}$ diameter beam (Bunton et al., 2007). There have been major increases in data-collection rates (now 5×10^6 atoms min^{-1}), field of view ($3 \times 10^4 \text{ nm}^2$), and

mass-resolving power (1,500). During the first 35 years of APT, only metals were studied because the specimens needed high electrical conductivity for shaping the electric field and voltage pulsing of the evaporation rate. With the development of LEAP and the introduction of laser techniques, researchers have extended the analysis into a larger field of applications such as semiconductors, ceramics, and organic and biological materials (Kelly & Larson, 2012).

Specimens for APT consist of a sharp needle with a tip of radius about 100 nm and a shank angle of 16° . This needle specimen geometry creates the high electric field necessary for field-induced evaporation. A particular feature of interest for APT must be located near the apex of a sharp tip, and specimen preparation is then a critical step in a successful measurement. Needle-shaped specimens have been prepared by electropolishing (Kelly & Larson, 2012). However, for many applications beyond the nano and atomic scale, focused ion beams (FIB)-based site-specific specimen preparation is required.

Here we report the specimen preparation method based

on FIB, describing general procedures as well as advanced applications to nanowires and nanopowders. We also introduce the arbitrarily rotation holders with moveable pin and an axial rotation manipulator to control the orientation of specimens.

MATERIALS AND METHODS

We first deposited a selected metal coating on the sample surface by ion beam sputtering (IBS; South Bay Technology Inc., USA). Next, an atom probe sample was prepared by lift-out techniques, using a dual-beam FIB (Nova Nanolab 600; FEI Inc., USA). The ion beam column in this instrument permits Ga^+ ion beam milling at 5~30 kV. Lift-out techniques were performed using a piezoelectric manipulator made by Kleindiek (MM3A) installed in the FIB system. The free lift-out specimen is positioned on a Si microtip by Pt deposition in the FIB. An array of Si posts (Micro Tip arrays, coupon; CAMECA, USA) (Larson et al., 2013) is also commercially available (Gault et al., 2012). This specimen is loaded on the chamber of atom probe equipment. An ultra-violet laser (wavelength, 355 nm) equipped with a laser-assisted local-electrode atom probe (LEAP 4000 \times HR; AMETEK, USA) was employed for assisting the evaporation of SiO_2 and providing a directionality of evaporated ions. The laser pulse repetition rate and laser power were 100 kHz and 200 pJ, respectively. The base temperature of the tip was reduced to 50 K during measurements. Three-dimensional reconstruction of APT data was performed using the analysis software (IVAS 3.6.6; AMETEK). We used an aluminum holder for holding the tungsten tip, which can be controlled to a full 360 $^\circ$ rotation. A G-1 epoxy kit (Gatan Inc., USA) was used for sample preparation with nanoparticles. The standard ratio of hardener to resin of 1:10 is used, giving a hardening time of about 10 minutes at 120 $^\circ\text{C}$; hardening of the epoxy is indicated by a yellow to brown color change.

RESULTS AND DISCUSSION

Specimen preparation for APT must address several key points: adequate field strength for field-induced evaporation, a uniform field, and successful measurement-yield. First, a radius of curvature between approximately 50 and 150 nm at the specimen apex is required. Second, the feature of interest needs to be within 100 nm of the specimen apex. Third, an appropriate shank angle of about 16 $^\circ$ is needed for heat escape. Specimen preparation using FIB techniques is a good means of making a sharp needle bearing a sample and satisfying these requirements.

Fig. 1 shows an example of typical specimen preparation for APT analysis, using Si microtip arrays. We used the SiO_2 with thickness of 200 nm on the Si substrate for specimen

preparation of APT. In order to reduce the damage on the sample surface during FIB preparation, Cr and Ni layers are commonly used with a thickness of 100 nm by IBS. This protective layer must be carefully selected with considering the feature of interest, its adhesive property, and the surface structure of the sample. A region of interest (ROI) in the bulk sample was identified using scanning electron microscopy. We deposited platinum for protecting layer of the surface by e-beam irradiation (Pt-EBID) at a stage tilting angle of 0 $^\circ$ and then by ion-beam irradiation (Pt-IBID) at a stage tilting angle of 52 $^\circ$, to form a layer about 3 μm wide, 20 μm long, and 300 nm thick on the ROI, as shown in Fig. 1A. The lift-out technique has become a popular method of preparing transmission electron microscopy (TEM) specimens and these samples are commonly milled at 52 $^\circ$. For an APT tip, however, a stage tilting angle of 22 $^\circ$ was required in this case to make a wedge-shaped specimen in Fig. 1B. This wedge shape is crucial for increasing the contact area between the Si flat-topped surface of the post and the sample for Pt coating (Thompson et al., 2007). We lift out this wedge sample using a tungsten-tip manipulator and put it onto the Si post, as shown in Fig. 1C and D, respectively. The wedge sample and Si post are joined by Pt-IBID, as shown in Fig. 1E and F. A key point during the lift-out procedure is to position the ROI on the center of the Si post. Fig. 1G-I show an annular milling procedure, using a stage tilting angle of 52 $^\circ$, which means that the ion beam and the longitudinal tip direction are parallel each other. An acceleration voltage of 30 kV was used, and the outer diameter of the circle pattern generated by beam rastering was held at 6 μm . The inner diameter (ID) and beam current were changed in three steps, with different magnifications for the electron beam used for observation. In the first step, the ion beam current was 3 nA and the annulus ID was 2.5 to 1.5 μm , and a magnification of 12,000 \times was used, as shown in Fig. 1G. For the second step, the ion beam current was reduced to 0.3 nA and the ID to 1.5 to 0.8 μm with a magnification of 20,000 \times (Fig. 1H). In the third step, the ion beam current was 30 pA and the ID, 800 to 200 nm with a magnification of 50,000 \times (Fig. 1I). The ROC at the tip apex was under 100 nm. Final cleaning and sharpening of the tip was performed at a low acceleration voltage of 2 to 5 kV at a stage tilting angle of 52 $^\circ$. Low acceleration voltages in the final step reduce the extent of Ga^+ penetration and is able to control the shank angle (Kato, 2004). The crucial aim of the annular milling procedure is to position the ROI within 100 nm of the end. In some specimens, such as thin films consisting of various materials, the sputter properties of different regions can produce large differences. This often creates a nonuniform apex on the specimen, since the ROI is preferentially milled away depending on the sputter yields of different components. In this case, keeping the ion-beam energy low with a current of 30 pA at 10 or 20 kV helps

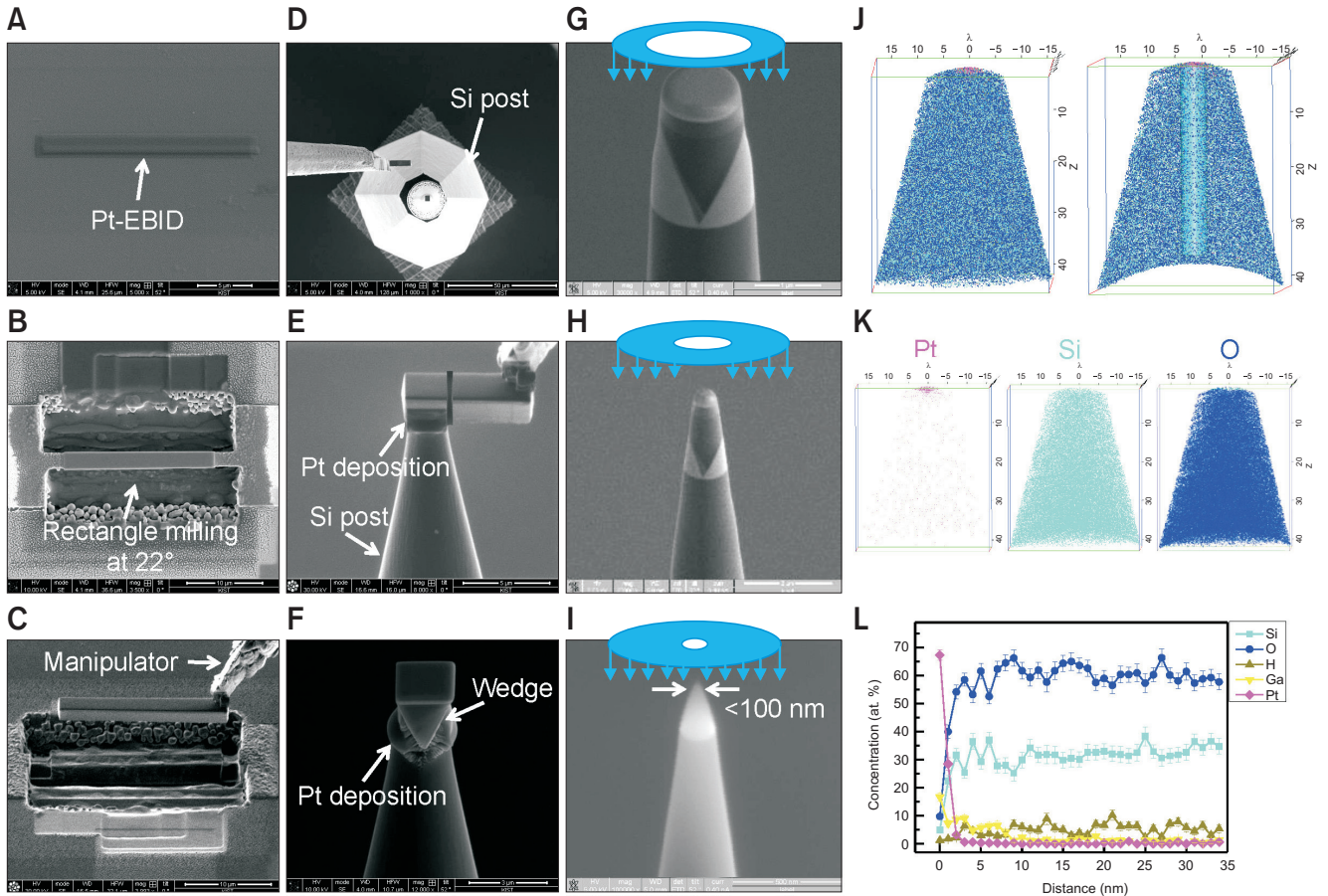


Fig. 1. Scanning electron microscopic images of specimen preparation for atom probe tomography (APT) analysis. (A) Pt deposition on the region of interest by e-beam induced deposition. (B) Coarse milling at a tilting angle of 22° using a rectangular pattern. (C) Lift-out of a lamella. (D) Transfer of a lamella to the Si micropost. (E) Pt deposition for joining the lamella and Si micropost. (F) Original wedge shape of the lamella before annular milling. (G) The first annular milling pattern. (H) The second milling pattern, producing a more tapered and narrowed end. (I) The final tip shape after a 2 to 5 kV ion cleaning step. (J) Left: Typical three-dimensional reconstruction image with $41 \times 34 \times 33 \text{ nm}^3$ from APT analysis of the SiO_2 . Right: The cylindrical region with volume of $5 \times 5 \times 33 \text{ nm}^3$ was selected for chemical composition analysis in the 7 nm-sliced reconstruction image. (K) Three-dimensional atom maps of Pt, Si, and O. (L) One-dimensional concentration profile of Si, O, Pt, Ga, and H through the cylindrical region in the right side of Fig. 1J.

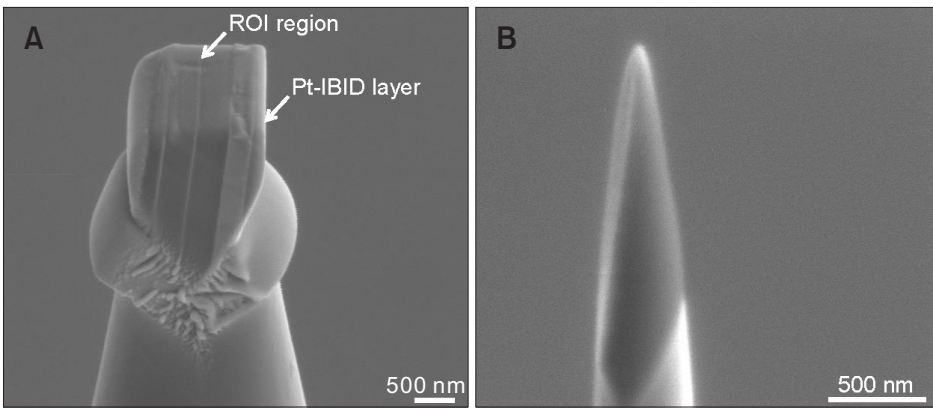


Fig. 2. Scanning electron microscopic images of a multi-layer thin film vertically loaded on the Si micropost for the interface atom probe tomography analysis; before (A) and after (B) annular milling. ROI, region of interest.

to make a good hemispherical apex (Felfer et al., 2012). We performed LEAP analysis in Fig. 1J-L with the SiO_2 tip of Fig. 1I. The left image of Fig. 1J shows a typical three-

dimensional reconstruction image with volume of $41 \times 34 \times 33 \text{ nm}^3$. The cylindrical region with volume of $5 \times 5 \times 33 \text{ nm}^3$ was selected for chemical composition analysis in the 7-

sliced reconstruction image in the right side of Fig. 1J. Fig. 1K shows three-dimensional elemental maps of Pt, Si, and O, respectively. The Pt was deposited to protect the top layer of sample from Ga ion milling. The Si and O were uniformly distributed. One-dimensional concentration profile was obtained through the cylindrical region in the right image of Fig. 1J. The compositional ratio of silicon to oxygen was approximately 1:2, which was well matched with their stoichiometry.

Thin films are generally positioned in a plane vertical to the

tip axis because the evaporation rates of the individual layers are different. There are some special cases, where there is weak adhesion, and the ROI must be in a plane parallel to the tip axis. The interface between layers is seen as a line (contrast difference) at the center of the specimen in Fig. 2.

Fig. 3A-F and 3G-I show the backside milling holder of 180° and a 90° rotation holder, respectively. We use a pin-type aluminum holder with tungsten tip attached. For backside milling, we first attached the cross-section specimen to the tungsten tip on the aluminum holder, as shown in Fig. 3A.

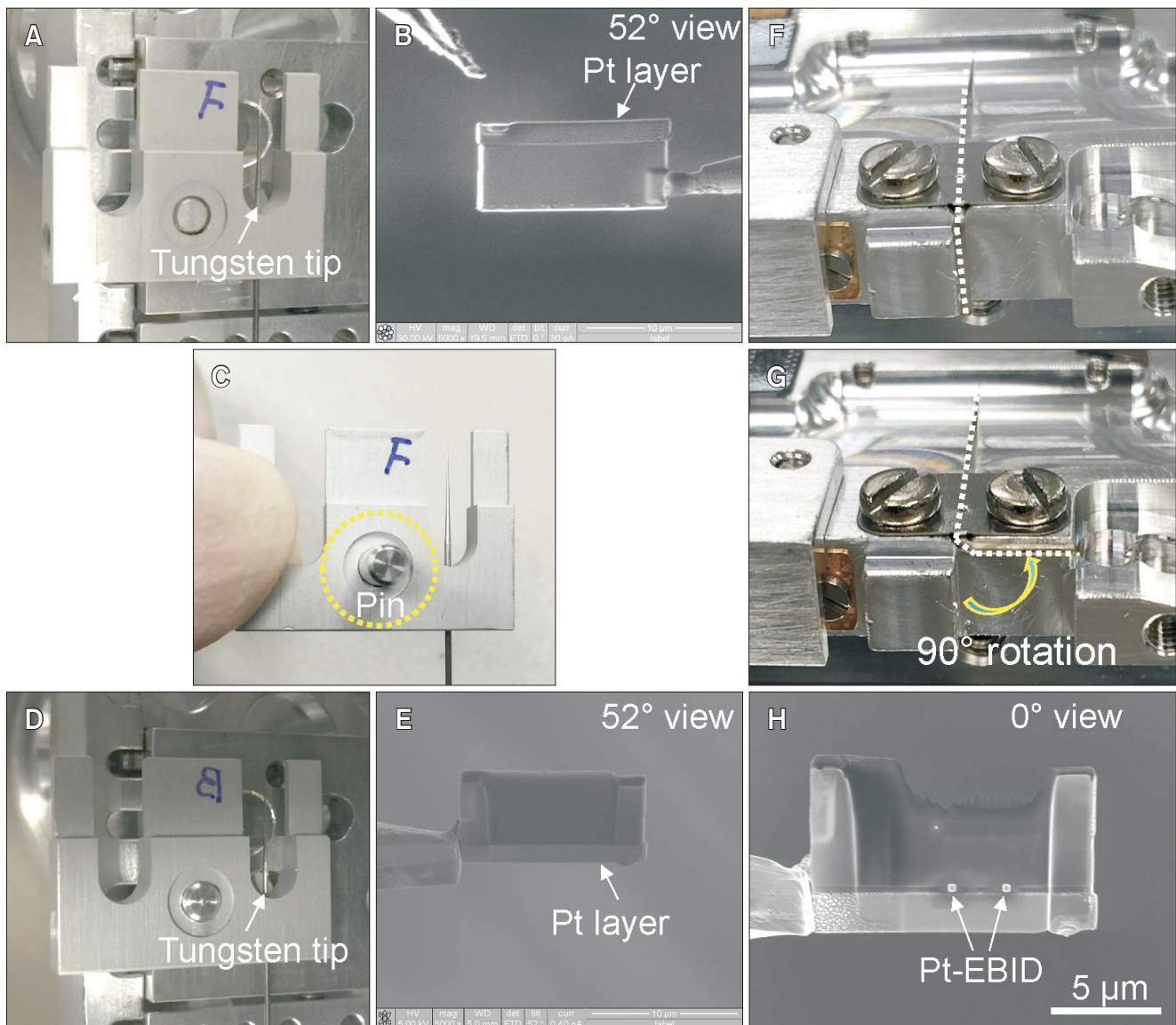


Fig. 3. Sample holder with tungsten tip for changing the specimen direction to the backside and 90°. (A) An aluminum holder with a tungsten tip. (B) 52° tilting view of scanning electron microscopy (SEM) image, using the setup in Fig. 3A. The Pt layer is on the upper surface. (C) Pin is pulled to the front for overturning a holder, as shown in the yellow circle. (D) The opposite side of the aluminum holder of Fig. 3A. (E) SEM image of the specimen in Fig. 3D. The Pt layer is located on the lower surface. (F) axial rotation manipulator of CAMECA holder. (G) Tungsten tip is rotated by 90°, as shown in the yellow arrow. (H) Normal view of SEM image of the specimen setup in Fig. 3G. We deposited the Pt-EBID on the target area at a stage tilting angle of 0° for marking the region of interest.

The deposited layer of Pt is originally on the top part in the initial stage, as shown in Fig. 3B. The pin is now pushed to reverse the orientation, as shown in Fig. 3C. The aluminum holder can be simply inverted to the backside orientation by changing the pin direction. Fig. 3D shows the opposite side of Fig. 3A after changing pin orientation. The deposited layer of Pt is located on the bottom for backside milling through turning the holder upside down, as shown in Fig. 3E. Fig. 3F-H shows the 90° rotation of the holder, changing the direction of the tungsten tip with the cross-section specimen. The specimen lifted out from the bulk sample is positioned at the end of the tungsten tip on a 90° rotation holder, as shown in Fig. 3F. The specimen attached at the end of the tungsten tip can be easily rotated to a 90° with this holder, as shown in Fig. 3G. We were able to observe the ROI region in the cross-section and deposited the Pt by EBID method on the ROI region, which is marked “Pt-EBID”, as shown in Fig. 3H. The technology of FIB-based specimen treatments has dramatically improved. However, APT sample preparation is still especially challenging for nanowires and nanoparticles. Only a few papers demonstrate procedures for nanowires (Allen et al., 2008; Blumtritt et al., 2014; Eichfeld et al., 2012; Lauhon, 2009; Perea et al., 2006); we will briefly describe

such preparation methods here. A manipulator is employed to detach a nanowire from a substrate, as shown in Fig. 4A-C. For an APT investigation, we choose a nanowire with a diameter under 100 nm, and then fix an end to the tungsten tip by Pt-EBID. The nanowire is subsequently pulled out from the substrate. The end of the nanowire is cleaned with a low accelerating voltage of 2 to 5 kV. In this case, it is necessary to maintain a good alignment of the tungsten tip and nanowire. There are some approaches for making an atom probe (AP) specimen with nanopowder, such as the atomic layer deposition method (Larson et al., 2015) and electro-deposition (Felfer et al., 2015). In powdered material, there are many pores for making an AP wedge sample using large particles, as shown in the cross-sectional image of Fig. 4D. As an alternative, we describe here a method using G-1 epoxy resin, which is commonly used in TEM specimen preparation. This resin forms a very thin glue film and is very hard after polymerization. It is also stable under electron and ion beam irradiations. We embedded nanoparticles in G-1 epoxy resin, and the encapsulated nanopowders were cured at ~60°C for 1 hour, after which they are easily handled and milled to prepare an APT specimen, as shown in Fig. 4E and F. The sampling procedure after embedding by epoxy resin is same

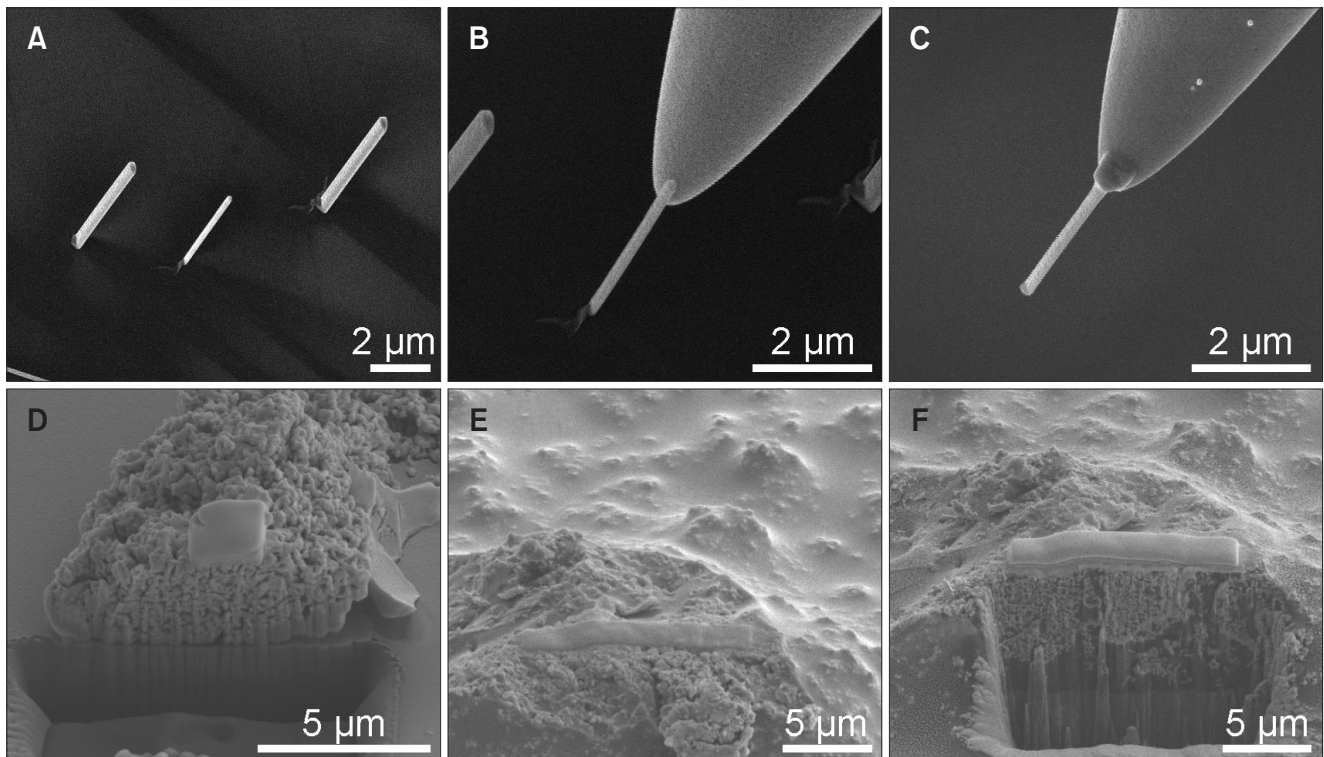


Fig. 4. Scanning electron microscopy (SEM) images of a pick-up method for nanowires and an embedding method for nanopowders. (A) Nanowires grown on a substrate with 45° elevation. (B) A nanowire is contacted to the tungsten tip by electron beam induced platinum deposition. The longitudinal axis of the tungsten tip and the nanowire should be parallel. (C) SEM image of the nanowire attached on the tungsten tip. (D) The cross-sectional image of a coarse powder with pores. (E) Normal view of SEM image of the nanopowder sample, which is embedded in G-1 epoxy resin. (F) The cross-sectional SEM image of the nanopowder embedded in epoxy resin, which is available general specimen preparation.

as the general FIB-based sample preparation in Fig. 1.

CONCLUSIONS

In three-dimensional reconstruction from APT data, the quality of the APT specimen becomes a limiting factor. In this work, we demonstrated a general procedure to fabricate APT specimens with a FIB-based method, using bulk samples, multi-layer thin films, nanowires, and nanopowders. There are general requirements for specimens for successful APT measurements. Firstly, the radius of curvature at the specimen apex must be in the range from approximately 50 to 150 nm. Secondly, the feature of interest (ROI) must be within approximately 100 nm of the specimen apex. Thirdly, an appropriate shank angle of about 16° is needed for heat escape. In the general FIB procedure we describe, the key

point during the lift-out procedure in specimen preparation from a bulk sample is positioning of the ROI on the center of the Si post. In shaping the specimen tip to achieve the needed radius of curvature, annular milling is used and the ROI is also set within 100 nm of the top end. We described the arbitrarily rotation holders with moveable pin and an axial rotation manipulator for changing sample direction to the backside and perpendicular direction. The lift-out specimen can be easily rotated using these holders. We also described a pick-up method for samples prepared from nanowires, and an embedding method for nanopowders.

CONFLICT OF INTEREST

No potential conflict of interest relevant to this article was reported.

REFERENCES

- Allen J E, Hemesath E R, Perea D E, Lensch-Falk J L, Li Z Y, Yin F, Gass M H, Wang P, Bleloch A L, Palmer R E, and Lauhon L J (2008) High-resolution detection of Au catalyst atoms in Si nanowires. *Nat. Nanotechnology* **3**, 168-173.
- Blumtritt H, Isheim D, Senz S, Seidman D N, and Moutannabbir O (2014) Preparation of nanowire specimens for laser-assisted atom probe tomography. *Nanotechnology* **25**, 435704-1-7.
- Bunton J H, Olson J D, Lenz D R, and Kelly T F (2007) Advances in pulsed-laser atom probe: instrument and specimen design for optimum performance. *Mirosc. Microanal.* **13**, 418-427.
- Eichfeld C M, Gerstl S S A, Prosa T, Ke Y, Redwing J M, and Mohney S E (2012) Local electrode atom probe analysis of silicon nanowires grown with an aluminum catalyst. *Nanotechnology* **23**, 215205-1-6.
- Felfer P, Li T, Eder K, Galinski H, Magyar A P, Bell D C, Smith G D W, Kruse N, Ringer S P, and Cairney J M (2015) New approaches to nanoparticle sample fabrication for atom probe tomography. *Ultramicroscopy* **159**, 413-419.
- Felfer P J, Alam T, Ringer S P, and Cairney J M (2012) A reproducible method for damage-free site-specific preparation of atom probe tips from interfaces. *Micro. Res. Tech.* **75**, 484-491.
- Gault B, Moody M P, Cairney J M, and Ringer S P (2012) *Atom Probe Microscopy*, p. 87, (Springer-Verlag New York, New York).
- Kato N I (2004) Reducing focused ion beam damage to transmission electron microscopy samples. *J. Elect. Microsc.* **53**, 451-458.
- Kelly T F, Bribb T T, Olson J D, Martens R L, and Shepard J D (2004) First data from a commercial local electrode atom probe (LEAP). *Microsc. Microanal.* **10**, 378-383.
- Kelly T F and Larson D J (2012) Atom probe tomography. *Annu. Rev. Mater. Res.* **42**, 1-31.
- Larson D J, Giddings A D, Wu Y, Verheijen M A, Prosa T J, Roozeboom F, Rice K P, Kessels W M M, Geiser B P, and Kelly T F (2015) Encapsulation method for atom probe tomography analysis of nanoparticles. *Ultramicroscopy* **159**, 420-426.
- Larson D J, Prosa Ty J, Ulfing R M, Geiser B P, and Kelly T F (2013) *Local Electrode Atom Probe Tomography* (Springer-Verlag New York, New York). p. 30.
- Lauhon L J (2009) Direct measurement of dopant distribution in an individual vapour-liquid-solid nanowire. *Nat. Nanotechnol.* **4**, 315-319.
- Perea D E, Allen J E, May S J, Wessels B W, Seidman D N, and Lauhon L J (2006) Three-dimensional nanoscale composition mapping of semiconductor nanowires. *Nano Lett.* **6**, 181-185.
- Thompson K, Lawrence D, Larson D J, Olson J D, Kelly T F, and Gorman B (2007) In situ site-specific specimen preparation for atom probe tomography. *Ultramicroscopy* **107**, 131-139.